CATALYST AND REACTOR DEVELOPMENT FOR A LIQUID PHASE FISCHER-TROPSCH PROCESS. QUARTERLY TECHNICAL PROGRESS REPORT, 1 OCTOBER 1983-31 DECEMBER 1983

ORIGINAL

AIR PRODUCTS AND CHEMICALS, INC.
ALLENTOWN, PA

JAN 1985

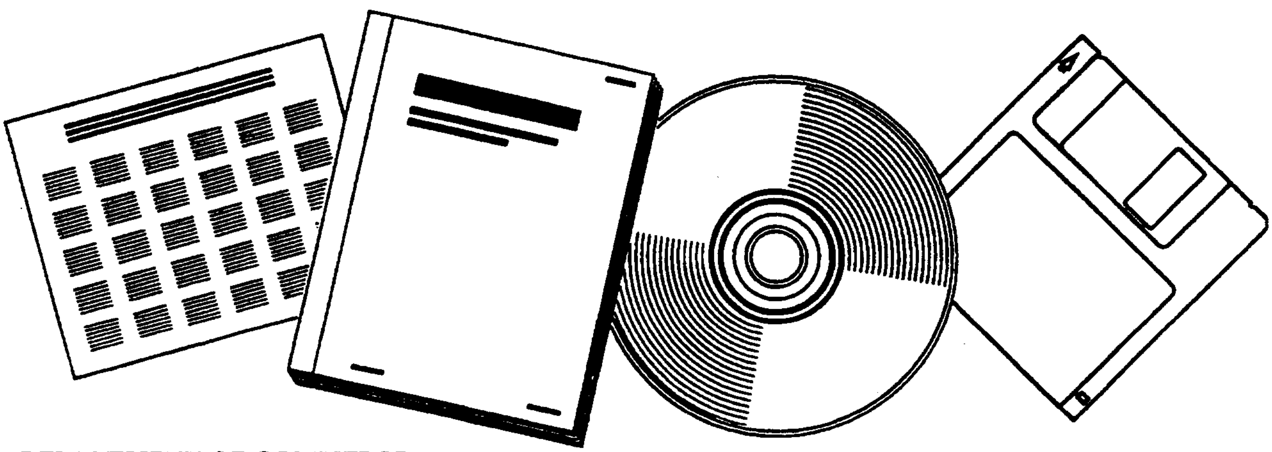

U.S. DEPARTMENT OF COMMERCE
National Technical Information Service

DOE/PC/30021-T16
(DE85005894)
Distribution Category UC-90d

CATALYST AND REACTOR DEVELOPM...

FOR A LIQUID PHASE FISCHER-TROPSCH

PROCESS

QUARTERLY TECHNICAL PROGRESS REPORT

FOR PERIOD 1 OCTOBER 1983 - 31 DECEMBER 1983

BARRY W. BRIAN
W. EAMON CARROLL
NELLIE CILEN
RONALD PIERANTOZZI
ANDREW F. NORDQUIST

AIR PRODUCTS AND CHEMICALS, INC.
ALLENTOWN, PA 18105

PREPARED FOR UNITED STATES DEPARTMENT OF ENERGY
UNDER CONTRACT NO. DE-AC22-80PC30021

EXECUTIVE SUMMARY

Two major tasks continued in the thirteenth quarter of the Air Products and Chemicals, Inc./U.S. Department of Energy Contract, "Catalyst and Reactor Development for a Liquid Phase Fischer-Tropsch Process": (1) Slurry Catalyst Development, and (2) Slurry Reactor Design Studies. In addition, work, as part of a three month contract modification, was begun to develop and improve the activity and center the selectivity for diesel fuel products of a proprietary catalyst A. This catalyst was found to produce yields in the diesel fuel region equal to or greater than the Schulz-Flory maximum with low rates of deactivation and good stability during previous extended periods of testing.

A phase two extended slurry test of a proprietary catalyst B was completed this quarter. A considerable improvement in activity was observed, making this batch nearly four times as active as in the first phase of testing. The selectivity for total, gasoline and diesel, fuels was over 65 wt% in both phases of testing. The results of this test show the importance of metals loading and the need for further development work to optimize the activity and selectivity for diesel fuel of this catalyst.

A short term (21 day) slurry test was conducted on another modified catalyst optimized by the gas phase screening program. Parametric gas phase screening tests were conducted on three additional catalysts. The optimum preparation and activation methods for diesel fuel selectivity will be chosen as these tests are completed.

Catalyst preparation for the contract modification was begun with the objective of determining the effect of promoter levels on activity and product selectivity.

In the hydrodynamic studies, work in the 12 inch Cold-Flow Simulator was completed. The following observations and/or conclusions were obtained:

- A Box-Behnken experimental design was utilized to determine the statistical significance of the independent parameters studied (superficial gas velocity, solids weight fraction, solid size, etc.) on gas holdup, as well as, any synergistic effects. Correlations for gas holdup in the 12 inch and 5 inch columns were obtained. In each column, a strong linear dependence on superficial gas velocity was obtained.

- A number of solid particle size ranges were studied in isoparaffin to determine the effect of size on the solids concentration profile along the bubble column. The smallest particle size range, 0.5-5 μm, gave the most uniform distribution.

- Bubble diameter data were obtained for iron oxide/isoparaffin using the hot film double conical probe. Average and Sauter mean bubble diameters, average bubble rise velocity, and gamma distribution parameters were obtained. For a wide range of operating conditions, the Sauter mean bubble diameter size remained in a fairly narrow range of 0.22 to 0.35 cm.

- Viscosity measurements on a typical Fischer-Tropsch wax from an extended slurry test were obtained as a function of temperature and a correlation derived.

An equation for optimum gas holdup, as a function of the intrinsic rate of reaction, solids loading, mass transfer rate, and Sauter mean bubble diameter was obtained. The sensitivity of space time yield to each of these parameters will be studied and optimum values obtained for bubble column operation.

TABLE OF CONTENTS

LIST OF TABLES

LIST OF FIGURES

1.0 INTRODUCTION

Coal liquefaction will be an important source of transportation fuels in the future, and can be accomplished by both a direct route (hydrogenation of coal in a donor solvent) or by an indirect route (gasification of coal followed by the Fischer-Tropsch reaction).

The product selectivity of the Fischer-Tropsch reaction has been the focus of extensive research for many years, yet still remains a prime target for technical innovation. Fischer-Tropsch technology, as it is currently practiced commercially for liquid fuels production, provides a broad range of hydrocarbon products which require costly downstream refining.

Selectivity can be influenced by variations in the catalyst composition and process conditions. Yet, in spite of the extensive effort devoted to this problem, a suitable catalyst has not previously been developed for producing a narrow range hydrocarbon product, such as gasoline or diesel fuel, without the coproduction of lighter and heavier undesirable products.

The Fischer-Tropsch reaction is exothermic, and improved heat transfer would also be expected to have a major beneficial effect on product selectivity. Slurry phase reactor operation improves heat transfer and temperature control, and results in greater selectivity to liquid products, usually through lower methane production. However, considerable differences have been reported in the space-time yield, catalyst life and ease of operation of slurry phase reactors.

In addition to improved product selectivity, slurry phase operation offers the advantage of ease of scale-up and the ability to directly utilize the carbon monoxide-rich synthesis gas produced by coal gasifiers. The full potential of the slurry phase Fischer-Tropsch process has not yet been realized, and its further development is an important part in our country's program to establish viable technology for converting coal to hydrocarbon fuels.

Air Products, under contract to DOE, has undertaken a program in catalyst and reactor development for a slurry phase Fischer-Tropsch process, and this report describes the work accomplished during the eleventh quarter.

2.0 OBJECTIVE

The overall objective of this program is to evaluate catalysts and slurry reactor systems for the selective conversion of synthesis gas into transportation fuels via a single stage, liquid phase process.

Task 1 - To establish a detailed Project Work Plan. This task was completed in the first quarter.

Task 2 - To evaluate and test catalysts for their potential to convert synthesis gas to gasoline, diesel fuel, or a mixture of transportation fuels suitable for domestic markets, and to quantify catalyst activity, selectivity, stability and aging with a target process concept involving a single stage, liquid phase reactor system.

Task 3 - To evaluate, through the use of cold flow reactor simulators, the flow characteristics and behavior of slurry reactors for the production of hydrocarbons from synthesis gas. This includes (1) defining heat, mass and momentum transfer parameters which affect the design of slurry reactors, (2) establishing operating limits for slurry reactors with respect to system physical parameters, (3) developing or confirming correlations for predicting the flow characteristics and heat/mass transfer of slurry reactors, and (4) defining the necessary requirements for the design of larger scale reactors.

Task 4 - To develop a preliminary design for a bench scale slurry phase Fischer-Tropsch reactor.

Tasks 5, 6, and 7 - To develop and improve the performance of catalyst A. The specific objectives are (1) to determine the critical factors controlling the activity and product selectivity of this catalyst and in so doing (2) increase its activity, and (3) center its selectivity to maximize diesel fuel production.

3.0 SUMMARY AND CONCLUSIONS

3.1 Task 2 - Slurry Catalyst Development

3.1.1 Sub-Task 2a - Background Studies

A computerized survey of available literature and patents dealing with the conventional and slurry phase Fischer-Tropsch processes, and the hydrodynamics of three phase slurry reactors, was continued.

3.1.2 Sub-Task 2c - Catalyst Preparation and Slurry and Gas Phase Reactor Testing

This section contains potentially patentable material and has, therefore, been issued in a supplementary report marked "Not for Publication".

3.2 Task 3 - Slurry Reactor Design Studies

Final gas holdup measurements in the 12 inch Cold Flow Simulator (CFS) were obtained on the iron oxide/isoparaffin system over a range of particle sizes, without heat transfer internals. The data agree well with the Akita and Yoshida[1] correlation as illustrated in Figure 1.

A Box-Behnken experimental design was employed to analyze the effects of the eight independent variables listed in Table 1, as well as their synergistic effects, on gas holdup. An exponential model was developed relating gas holdup to four parameters:

$$\alpha/(1-\alpha)^4 = 0.483\ Vg^{1.03}/(\rho_{SL}{}^{2.26} HS^{0.058} V_L{}^{0.049}) \qquad (1)$$

$(R^2 = 0.91)$

$\rho_{SL} = \rho_L/[1 - WT(1-\rho_L/\rho_S)]$ = Slurry density, g/cm^3

ρ_S = Solid density, g/cm^3

V_g = Superficial gas velocity, ft/sec

V_L = Liquid velocity, ft/sec

HS = Distributor hole size, in

A similar correlation was obtained using the 5 inch CFS data:

$$\alpha/(1-\alpha)^4 = 0.36\, V_g^{0.96} dp^{0.10}/WT^{0.27} \qquad (2)$$
$$(R^2 = 0.94)$$

In both the 12 inch and 5 inch columns, the same linear dependence on superficial gas velocity was obtained. Also, the effect of solids loading was similar, i.e., an increase in solids concentration lead to decreased gas holdup. The distributor hole size and liquid velocity did not have a significant affect on gas holdup and as such do not appear in the 5 inch CFS correlation. Equation 1 will be used in subsequent bubble column computer simulations.

Solid concentration profiles were measured for a number of iron oxide particle size ranges in isoparaffin. The conclusion of these tests, as determined previously, was that particle size is the primary determinant for solids distribution with the smallest particle size giving the most uniform profile.

Bubble diameter measurements were completed for the iron oxide/ isoparaffin system using the hot film double conical probe. As illustrated in Table 2, the uncorrected bubble diameters remained relatively constant over the entire range of operating conditions. After calibrations were conducted for lag and dwell times, the Sauter mean bubble diameters were found to be in the range 0.22-0.35 cm as illustrated in Table 3. Thus, given a reliable correlation for gas holdup, it is possible to obtain a reliable correlation for interfacial area by the equation:

$$a = 6\alpha / d_B \qquad (3)$$

Because of the lower surface tension of the isoparaffin medium and higher observed gas holdup, it can be reasonably argued that in isoparaffin the bubble diameter should be smaller than in water. The lower end of the bubble size range agrees well with the Calderbank[2] correlation which predicts a Sauter mean bubble diameter of 0.23 cm at Fischer-Tropsch operating conditions. This approximate size was also confirmed by photographic stuc conducted in Task 3 on the 5 inch CFS. The following interfacial area correlation will be used for determining the gas to liquid mass transfer coefficient in a bubble column:

$$a = 6\,\alpha/0.23 = 26.09 \qquad (cm^2) \tag{4}$$

Viscosities of Fischer-Tropsch wax obtained from an extended catalyst run, were measured as a function of temperature by an outside contractor. The data is plotted in Figure 1. In addition, viscosities of a 20 and 30 wt% loading of 0.5 to 5 μm Fe_2O_3/wax slurries were measured at 260°C and are included in Figure 1. For comparison, values from a Deckwer correlation [3] are also plotted. Correlating the liquid viscosity data using the de Guzman-Andrade relation gave:

$$\mu_L = \exp\,(2399/T - 8.115) \quad (R^2 = 1.00) \tag{5}$$

This is very similar to the correlation used by Deckwer:

$$\mu_L = \exp\,(3266/T - 9.862) \tag{6}$$

The Air Products' correlation has been incorporated into the Deckwer bubble column simulation model.

Using kinetic rate expressions for hydrogen consumption at the catalyst surface coupled with the rate of hydrogen transport across the gas-liquid interface, results in an equation describing the rate of hydrogen consumption as a function of the intrinsic reaction rate, the catalyst loading, the gas to liquid mass transfer rate, and Sauter mean bubble diameter. The derivative of this expression may then be taken with respect to gas holdup and set equal to zero to obtain the optimum gas holdup to maximize the reaction rate or the space time yield in a bubble column:

$$\alpha\ \text{opt} = 1/[1 + (6K_L(1 + U)/K_o w d_B)^{1/2}] \tag{7}$$

Table 4 summarizes the results for α opt for some Air Products catalysts. Note the sensitivity of α opt on bubble diameter; a doubling of gas holdup is required to offset a threefold increase in bubble size. The superficial gas velocity and space time yield were calculated using the Air Products' correlation for gas holdup and Deckwer's bubble column simulator for the five cases in Table 4.

3.3 Tasks 5, 6, and 7 - Contract Modification

Activity in this task contains potentially patentable material and has, therefore, been described in the supplementary report marked "Not for Publication"

4.0 ACKNOWLEDGEMENTS

The contributions made to this program by P. A. Dotta, M. Louie, S. E. Madison and L. E. Schaffer are gratefully acknowledged.

5.0 RESULTS AND DISCUSSION

5.1 Task 2 - Slurry Catalyst Development

5.1.2 Sub-Task 2c - Catalyst Preparation and Slurry and Gas Phase Reactor Testing

This section contains potentially patentable material and has, therefore, been issued in a supplementary report marked "Not for Publication".

5.2 Task 3 - Slurry Reactor Design Studies

5.2.2 12 Inch Cold Flow Simulator

(i) Gas Holdup

Gas holdup measurements in the 12 inch Cold Flow Simulator (CFS) were obtained on the 0.5-5, 45-53, and 90-115 μm iron oxide/isoparaffin systems without heat transfer internals. The results, listed in Table 5 and illustrated in Figure 1, agree well with the Akita and Yoshida[1] correlation.

The independent variables in Table 1 were analyzed to determine their effects on gas holdup. In order to efficiently quantify the effects of these variables, a Box-Behnken experimental design was employed. The experimental design allows for each variable to be fit by a quadratic relationship. It also allows the effect of interactions, or synergistic effects, between two variables to be quantified. If every variable and interaction were statistically significant, the correlation would have 44 terms! Each of these 44 terms was analyzed and 6 of the 44 were found to be statistically significant. The following statistical correlation for predicting gas holdup in the 12 inch CFS was obtained:

$$\alpha = 0.0581 + (0.595 - 0.505V_G)V_G - 0.221\,WT + 0.002\,d_p + (0.333 - 0.007\,\rho_L)HS \tag{8}$$

with $R^2 = 0.88$

α = Gas holdup, volume fraction
V_G = Superficial gas velocity, ft/sec
WT = Solid weight fraction
d_p = Solid size, μm
ρ_L = Liquid density, lbm/ft^3
HS = Distributor hole size, in

Subsequent to this analysis, several improvements were made to the gas holdup analysis. A more accurate gas velocity value was determined taking into account the expansion and temperature drop of the gas through the orifice meter. A more accurate surface tension relationship incorporating the effect of solids loading on surface tension was also developed. Lastly, slurry density and viscosity were used instead of liquid properties. These improvements were used to fit the gas holdup correlation to an exponential model, equation (1):

$$\alpha/(1-\alpha)^4 = 0.483V_G^{1.03}/\rho_{SL}^{2.26}HS^{0.056}V_L^{0.049}$$

ρ_{SL} = $\rho_L/(1 - WT(1-\rho_L/\rho_S))$
$\rho_{SL,S}$ = Slurry density, solid, g/cm^3
V_g = Superficial gas velocity, ft/sec.
V_L = Liquid velocity, ft/sec
HS = Distributor hole sizes, in

For $V_L = 0$ experimental runs, a value of $V_L = 0.0001$ was used.

These improvements enabled gas holdup to be better described (having a higher R^2) using only four parameters instead of five parameters as in equation (8). Comparing equation (1) to the silicon oxide/aqueous correlation obtained in the 5 inch CFS, equation (2):

$$\alpha (1-\alpha)^{4} = 0.36V_{G}^{0.96}d_{p}^{0.10}/WT^{0.27}$$

we see that both correlations have the same linear dependence on gas velocity. Slurry density, ρ SL, incorporates solids loading only, therefore, ρ SL or WT appearing in each correlation show the same decrease in gas holdup with solids loading. Hole size was not a variable in the 5 inch CFS study, thus it does not appear in that correlation. Solid size appears in equation (8), but not in equation (1); its effect is small.

There are several advantages to fitting the data to a statistical model like equation (8). The statistical correlation shows that there is an interaction between the liquid (denoted by liquid density) and distributor hole size. This is not surprising since the two liquids studied have vastly different surface tensions. Surface tension, in turn, has an effect on the bubble size that a given distributor will produce. This interaction cannot be modelled by a linear exponential correlation. Also, the statistical correlation can easily handle zero values such as no solids or zero liquid velocity whereas the exponential model requires transformation. The transformation will tend to change the value of the exponents in the correlation. The exponential correlation has received wide acceptance and is, therefore, the one that is being employed in the bubble column computer simulation.

(ii) Solids Concentration Profiles

Solids concentration profiles were measured for the 0.5-5, 45-53, and 90-115 μm iron oxide/isoparaffin systems in the 12 inch CFS and are listed in Table 5 and illustrated in Figure 3. As shown previously, particle size was the major determinant of solids distribution. Also, the smaller the particle size range, the more uniform the solids distribution.

(iii) Bubble Diameter

Bubble diameters were obtained for the iron oxide/isoparaffin systems above using the hot film double conical probe. The average and Sauter mean bubble diameters, the average bubble rise velocity, and the gamma distribution parameters were obtained for all runs and are listed in Table 2. In spite of the wide range of operating conditions, the uncalibrated bubble diameter size range remained fairly narrow from 0.28 to 0.44 cm. The average bubble rise velocity was also in a very narrow range of 25.6 to 35.7 cm/sec. Both the uncorrected average bubble diameter and bubble rise velocity are slightly larger than that expected from the literature[4]. The reason for this is discussed by Rowe and Masson[5]. They observed that a probe shaped similar to the one used in this study caused bubbles to accelerate as they were transected. Probes, in general, also caused bubbles to elongate making measured chord lengths appear longer than they would be in an undisturbed bubble. It was, therefore, necessary to calibrate the bubble diameter probe; the calibration method is discussed in Section 6.2.

The calibration studies did show that smaller bubbles are slowed down to a much greater degree than larger bubbles. This effect accounts for the mean bubble sizes being smaller at the column center than at the column wall, contrary to expectation. The difference, however, is not statistically significant expect in run 86. The radial profile is less pronounced at the lower gas velocity, as expected.

The corrected Sauter mean bubble diameters, listed in Table 3, were in the 0.22 to 0.35 cm range. Calderbank[2] predicted a Sauter mean diameter of 0.23 cm at Fischer-Tropsch operation conditions. This approximate size was also confirmed by photographic studies conducted in Task 3 on the 5 inch CFS.

(iv) Fischer-Tropsch Wax Viscosity

Liquid viscosity of an actual Fischer-Tropsch wax, taken from the catalyst A extended test of the catalyst development program, was measured by Contraves AG of Zurich, Switzerland. The data are plotted as a function of temperature in Figure 2. To the liquid wax, 0.5-5 μm Fe_2O_3 was added to make a 20 wt% and 30 wt% slurry. The viscosity of these slurries were measured at 260°C and are included on Figure 2. For comparison, the Deckwer[3] correlation was also plotted on Figure 2 and appears to be in good agreement with the Air Products' catalyst-free data.

(v) Engineering Evaluation

In bubble column operation there exists an optimum gas holdup which will maximize column space time yield. Gas holdups higher than this optimum will be reaction rate limited while those lower than this will be mass transfer limited. The optimum gas holdup will be affected by bubble size, the intrinsic kinetic rate, catalyst weight loading, and the rate of mass transfer across the gas-liquid interface. In the slurry phase, the rate of hydrogen consumption at the catalyst surface expressed as:

$$r = r_{H_2} = r_{CO + H_2}/(1 + U)$$

$$= K_O w(1 - \alpha)C/(1 + U) \tag{9}$$

is equal to the rate at which hydrogen is transported across the gas-liquid interface:

$$r = K_L a\ (C^* - C) \tag{10}$$

Interfacial area, a, is related to gas holdup and bubble size by equation (3):

$$a = 6\ \alpha / d_B$$

Solving equation (10) for C and substituting it and equation (3) into equation (4), eliminates the hydrogen concentration in the liquid phase, C:

$$r = (6K_L C^*/d_B)\alpha/(1 + (6K_L(1 + U)/Kowd_B)\alpha/(1 - \alpha)) \quad (11)$$

To find the gas holdup, α, which allows for the maximum consumption rate of hydrogen, the derivative of equation (11) is taken with respect to α and the resulting expression is set equal to zero:

$$dr/d\alpha = 0 = (1 - 6K_L (1 + U)/K_0Wd_B)\alpha^2 opt - 2\alpha opt + 1 \quad (12)$$

Solving equation (12) quadraticly yields one physically realistic solution:

$$opt = 1/(1 + (6K_L(1 + U)/K_0wd_B)^{1/2}) \quad (13)$$

In equation (13) it is observed that increasing the intrinsic kinetic rate constant, the catalyst loading or the Sauter mean bubble diameter all result in increasing the optimum gas holdup value. Conversely, as the rate of mass transfer, K_L, increases, the optimum gas holdup decreases.

It is interesting to note that while C^*, the hydrogen solubility, directly increases the space time yield, it does not affect the optimum gas holdup value.

Using equation (13), the optimum gas holdup and resulting gas velocity for a variety of values of K_0, W, and d_B are given in Table 4. Going from a bubble size of 0.07 cm as measured by Deckwer[3] to 0.23 as used by Satterfield[6] results in roughly doubling of the optimum gas holdup value. Increasing the weight loading by a factor 3 results in roughly a 50% increase in the optimum gas holdup value. Thus, it is seen that K_0, W, K_L, and d_B all have an important affect on the reactor space time yield. The superficial gas velocity and space time yield were calculated, using Deckwer's bubble column simulator and Air Products' correlation for gas holdup, for the five cases listed in Table 4.

Nomenclature

a	— Interfacial area, cm^2 surface area cm^{-3} expanded slurry.
C	— Concentration of hydrogen gas in liquid phase, mol H_2 cm^{-3} slurry.
C^*	— Equilbrium concentration of hydrogen gas in liquid phase, mol H_2 cm^{-3} slurry.
CZ	— Probability of observing a bubble chord length less than λ.
d	— Mean bubble dimeter, cm.
d_B	— Sauter mean bubble diameter, cm.
K_L	— Mass transfer coefficient cm sec^{-1}.
K_0	— Intrinsic reaction rate, sec^{-1} wt%^{1}..
LT	— Lag time, sec.
N	— Molar consumption rate, mol sec^{-1}.
n,s	— Cumulative gamma distribution parameters.
r, r_{H_2}	— Rate of disappearance H_2, mol cm^{-3} slurry sec^{-1}.
r_{CO} + H_2	— Rate of disappearance CO + H_2, mol cm^{-3} slurry sec^1.
U	— N_{CO}/N_{H_2}, usage ratio.

V_R — Volume of expanded slurry, cm^3.

X, Y — Variables of integration.

W — Catalyst weight loading, wt%.

α — Gas holdup, volume fraction gas.

λ — Bubble chord length, cm.

6.0 EXPERIMENTAL

6.1 Task 2 - Slurry Catalyst Development

6.1.1 Sub-Task 2c - Catalyst Preparation and Slurry and Gas Phase Reactor Testing

This section contains potentially patentable material and has, therefore, been issued in a supplementary report marked "Not for Publication".

6.2 Task 3 - Slurry Reactor Design Studies

(i) Bubble Diameter

The double conical probe was calibrated in the plexiglas calibration chamber.

(a) Calibration Chamber Description

An isometric view of the plexiglas calibration chamber is shown in Figure 4. The chamber is roughly a 5 inch outer diameter cube. This shape minimized photographic aberration. The probe was inserted from the back face. The single bubble distributor could be inserted from either the bottom face or from the rear face. Pictures could be taken from either the front or top faces. A verticle reference stick denoting 1/64th inch was placed the same distance as the probe from the camera.

(b) Calibration Procedure

A GenRad Model 1531 stroboscope was used along with a polaroid camera with adjustable shutter speed and F stop to obtain stroboscopic pictures of a stream of bubbles impinging on the double conical probe. Adjusting the strobe 'froze' the bubble stream. Three to four bubbles were captured in the picture to obtain bubble rise velocities.

As the strobe frequency became an integer or half integer multiple of the bubble frequency, the action was frozen. It was important that the correct setting be used. Starting at a low strobe frequency, 300 rpms, the strobe rate was increased until freezing the action produced more bubbles in the picture than had been seen at the previous freeze frequency. The strobe was then dialed back down to that previous lower freeze point, and pictures were taken at that setting. The shutter speed was low enough to allow two strobe flashes.

Bubble rise velocities are calculated as follows:

$$V_B = SF(DX) \tag{16}$$

Where:

V_B = Bubble rise velocity, cm/sec

SF = Strobe frequency, sec^{-1}

DX = Distance between bubble tops, cm

The distance between bubble tops was measured because, for larger bubbles, bubble tops were not observed to deform.

It was necessary to place the gas sparger near enough to the probe to assure a consistent hit, about 3/4 inch. At this distance it was doubtful that the bubble had reached a steady state rise velocity. In spite of this, agreement with Calderbank data[2] was good.

The effect of the bubble probe in slowing down the bubble was greatly influenced by bubble size. The smallest bubble studied, 0.8 mm, was slowed down 20-25% upon hitting the probe. The largest bubble, 8 mm wide, experienced no reduction in velocity before and after hitting the probe. The intermediate bubble size of 2.2 mm h its velocity reduced roughly 10% before and after hitting the probe.

A representative bubble trace is shown in Figure 5. The beginning and end of each bubble was taken at the point in which the derivative of the trace changed sign. The larger the bubble, the clearer this transition.

7.0 REFERENCES

1. Akita, K. and F. Yoshida, Ind. Eng. Chem. Proc. Des. Dev., 1973, 12, 76.

2. Calderbank, P., et. al., "Catalysis in Practice", Symp. Proceed . Instr. Chem. E., 1963, 66.

3. Deckwer, W. D.; Louisi, Y.; Zakdi, A.; Ralek, M. Ind. Eng. Chem. Process Des. Dev. 1980, 19, 699.

4. Calderbank, P. H., S. L. Johnson, and J. London, Chem. Eng. Sci, 25, 1970, 235.

5. Rowe, P. N. , and H. Masson, Trans. I. Chem. E., 59, 1981, 177-185.

6. Satterfield, C. N. and G. A. Huff, Jr., Chem. Eng. Sci., 35, 1980, 195-202.

TABLE 1

INDEPENDENT VARIABLES IN 12" COLD FLOW SIMULATOR STUDY

SLURRY MEDIUM	:	PARAFFIN, WATER
SUPERFICIAL GAS VELOCITY	:	0.05 - 0.5 FT/SEC
SUPERFICIAL LIQUID VELOCITY	:	0 - 0.015 FT/SEC
SOLID	:	SILICA, IRON OXIDE
SOLID SIZE	:	1-5 μM, 45-53 μM, 90-106 μM
SOLID CONCENTRATION	:	0 - 30 WT%
HEAT TRANSFER INTERNAL TUBES	:	NONE, PLAIN, FINNED
DISTRIBUTOR HOLE SIZE	:	0.035, 0.125, 0.5 IN.

Table 2

Bubble Diameter - 12" Cold Flow Simulator

Run No.	Dist Hole in	Inter	Solid Oxide	Solid Size μm	Solid Avg wt%	Liq. Type	Velocity Slurry ft/sec	Velocity Gas ft/sec	Probe Loc * in	Uncorrected** Bubble Diameter Avg cm	Uncorrected** Bubble Diameter Sauter cm	Avg Vel cm/sec	Gamma Distribution a	Gamma Distribution n
83	0.035	Y	Fe	2.5	6.7	Iso	0.000	0.26	2	0.166	0.295	28.322	-15.4007	2.5500
84	0.125	Y	Fe	98	11.3	Iso	0.000	0.43	2	0.187	0.317	28.651	-15.4030	2.8744
85	0.125	Y	Si	2.5	29.4	Iso	0.008	0.16	2	0.193	0.322	25.659	-15.4039	2.9648
86	0.500	N	-	-	-	Iso	0.008	0.20	5	0.204	0.333	27.790	-15.4055	3.1355
									3	0.202	0.332	32.179	-15.4052	3.1064
									0	0.174	0.304	35.666	-15.4016	2.6783
87	0.035	N	Si	2.5	24.8	Iso	0.008	0.12	5	0.303	0.433	25.253	-15.4257	4.6776
									3	0.310	0.440	28.874	-15.4268	4.7840
									0	0.276	0.406	32.646	-15.4189	4.2553
88	0.035	N	Si	49	18.9	WA	0.008	0.50	5	0.203	0.333	27.298	-15.4054	3.1307
89	0.035	N	Si	49	18.5	WA	0.008	0.16	5	0.263	0.393	26.251	-15.4159	4.0532
93	0.125	N	Fe	2.5	15.6	Iso	0.0	0.22	2	0.206	0.336	30.560	-15.4057	3.1729
94	0.125	N	Fe	2.5	15.5	Iso	0.008	0.06	2	0.250	0.380	31.724	-15.4134	3.8575
95	0.500	N	Fe	49.0	21.3	Iso	0.008	0.30	2	0.219	0.349	29.336	-15.4079	3.3791
96	0.500	N	Fe	98.0	5.8	Iso	0.008	0.28	2	0.185	0.315	32.073	-15.4030	2.8436
97	0.035	N	Fe	98.0	23.1	Iso	0.015	0.55	5	0.203	0.333	26.727	-15.4054	3.1222
									3	0.183	0.313	28.161	-15.4024	2.8169
									0	0.154	0.284	28.626	-15.3994	2.3690

*Distance from column center

**Diameters not corrected for probe interference. Relative order will be the same. Absolute values will be smaller.

Table 3

Bubble Diameter - 12" Cold Flow Simulator

Run No.	Dist Hole in	Inter	Solid Oxide	Solid Size μm	Solid Avg wt%	Liq. Type	Velocity ft/sec Slurry	Velocity ft/sec Gas	Probe Loc * in	Corrected Bubble Diameter Avg cm	Corrected Bubble Diameter Sauter cm	Avg Vel cm/sec	Gamma Distribution a	Gamma Distribution n
83	0.035	Y	Fe	2.5	6.7	Iso	0.000	0.26	2	0.106	0.236	28.322	-15.4007	1.634
84	0.125	Y	Fe	98	11.3	Iso	0.000	0.43	2	0.124	0.254	28.651	-15.4030	1.905
85	0.125	Y	Si	2.5	29.4	Iso	0.008	0.16	2	0.128	0.258	25.659	-15.4039	1.967
86	0.500	N	-	-	-	Iso	0.008	0.20	5	0.137	0.266	27.790	-15.4055	2.103
									3	0.136	0.266	32.179	-15.4052	2.090
									0	0.113	0.243	35.666	-15.4016	1.745
87	0.035	N	Si	2.5	24.8	Iso	0.008	0.12	5	0.217	0.346	25.253	-15.4257	3.343
									3	0.222	0.352	28.874	-15.4268	3.340
									0	0.195	0.325	32.646	-15.4189	3.008
88	0.035	N	Si	49	18.9	WA	0.008	0.50	5	0.137	0.266	27.298	-15.4054	2.105
89	0.035	N	Si	49	18.5	WA	0.008	0.16	5	0.185	0.314	26.251	-15.4159	2.845
93	0.125	N	Fe	2.5	15.6	Iso	0.0	0.22	2	0.128	0.258	30.560	-15.4057	1.977
94	0.125	N	Fe	2.5	15.5	Iso	0.008	0.06	2	0.162	0.292	31.724	-15.4134	2.497
95	0.500	N	Fe	49.0	21.3	Iso	0.008	0.30	2	0.138	0.268	29.336	-15.4079	2.130
96	0.500	N	Fe	98.0	5.8	Iso	0.008	0.28	2	0.112	0.242	32.073	-15.4030	1.726
97	0.035	N	Fe	98.0	23.1	Iso	0.015	0.55	5	0.126	0.256	26.727	-15.4054	1.938
									3	0.111	0.240	28.161	-15.4024	1.702
									0	0.088	0.218	28.626	-15.3994	1.359

*Distance from column center

Table 4

Optimum Gas Holdup and Gas Velocity*

$K_L = 0.0205$ cm/s

$U = 2$

Case	K_O sec^{-1} $wt\%^{-1}$	w %	d_B cm	α opt vol %	V_G cm/sec	STY / STY 1
1	1.4×10^{-3}	20	0.07	6.8	2.13	1.00
2	1.4	60	0.07	11.2	12.75	2.72
3	6.1	60	0.07	20.9	36.43	9.42
4	1.4	20	0.30	13.1	5.29	0.87
5	1.4	60	0.30	20.7	36.00	2.17

*Using APCI cold flow gas holdup correlation.

Table 5

Gas Holdup and Solid Fraction: 12" Cold Flow Simulator[1]

Run No.	Dist. Hole (in.)	Solid Size (μm)	Avg. WT%	Velocity (ft/sec)		Gas Holdup (Vol. %)				Solid Fraction (WT%)			
				Slurry	Gas	1-2	2-3	3-4	Avg.	1	2	3	4
93	0.125	2.5	15.6	0.0	0.22	9.6	11.9	12.0	13.3	15.9	15.6	15.7	15.4
94	0.125	2.5	15.5	0.008	0.06	1.4	4.9	3.5	4.3	15.6	15.9	15.2	15.2
95	0.500	49.0	21.3	0.008	0.30	-	9.2	10.3	11.0	-	32.9	28.6	23.6
96	0.500	98.0	5.8	0.008	0.28	-	15.0	15.0	15.4	-	12.1	7.2	4.0
97	0.035	98.0	23.1	0.015	0.55	-	20.7	23.2	22.0	43.1	25.8	15.1	8.5

[1]Three-Phase System: Iron Oxide/Isoparaffin/Nitrogen

No heat transfer internals.

FIGURE 1

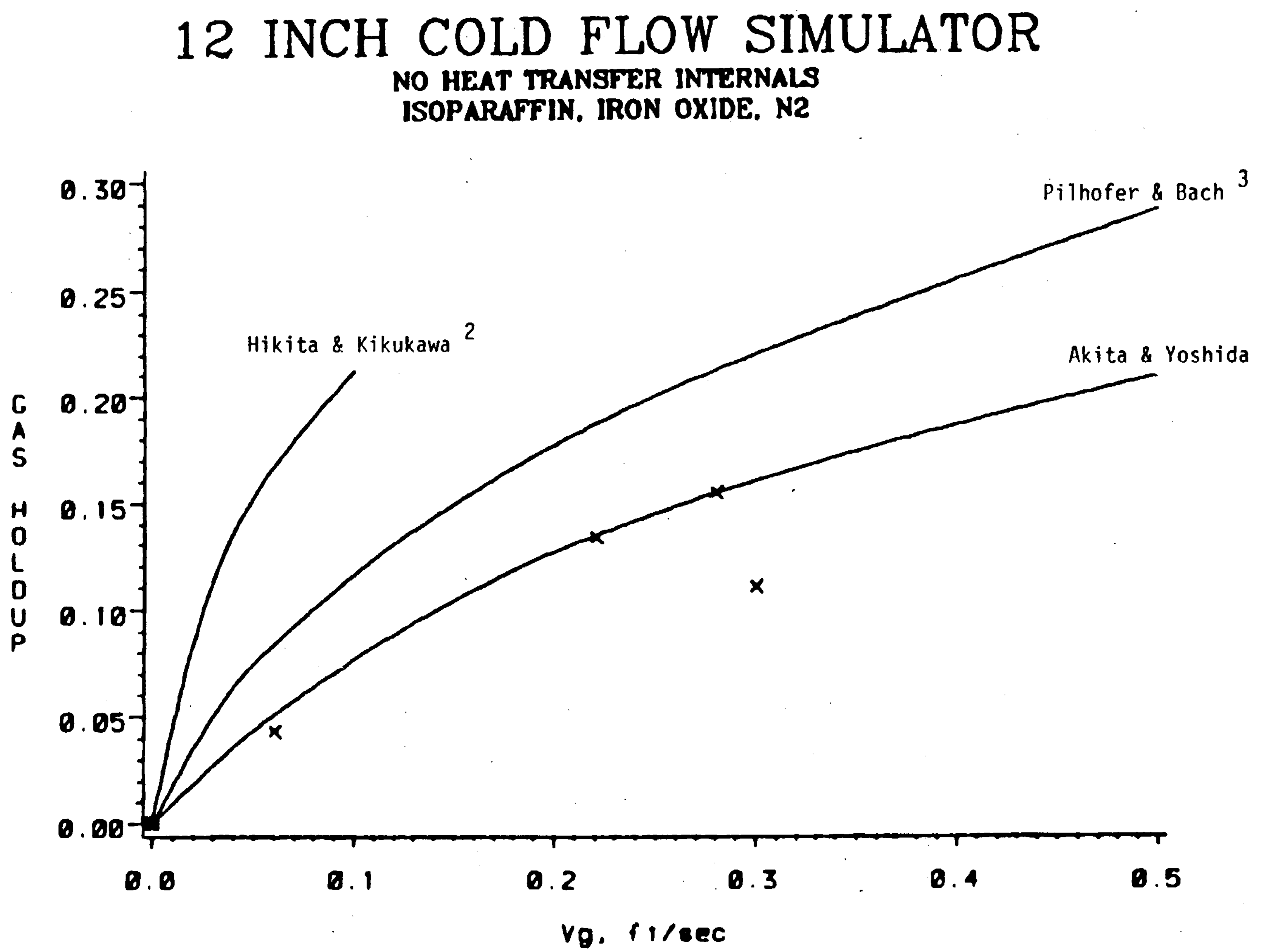
12 INCH COLD FLOW SIMULATOR
NO HEAT TRANSFER INTERNALS
ISOPARAFFIN, IRON OXIDE, N2
GAS HOLDUP
0.30
0.25
0.20
0.15
0.10
0.05
0.00
0.0
0.1
0.2
0.3
0.4
0.5
Vg, ft/sec
Hikita & Kikukawa 2
Pilhofer & Bach 3
Akita & Yoshida 1

Figure 2

Liquid Viscosity of Fischer-Tropsch Wax

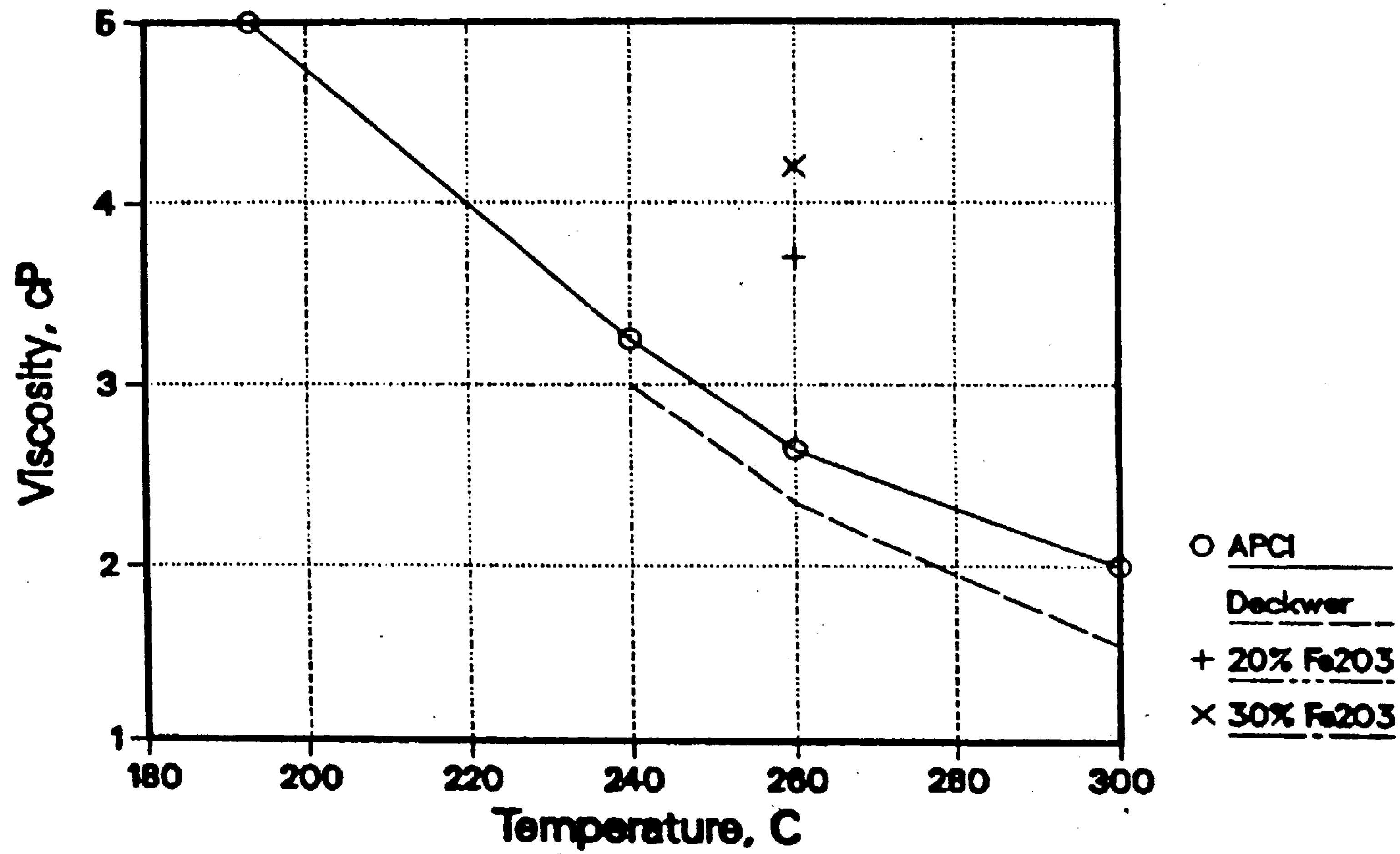

Figure 3

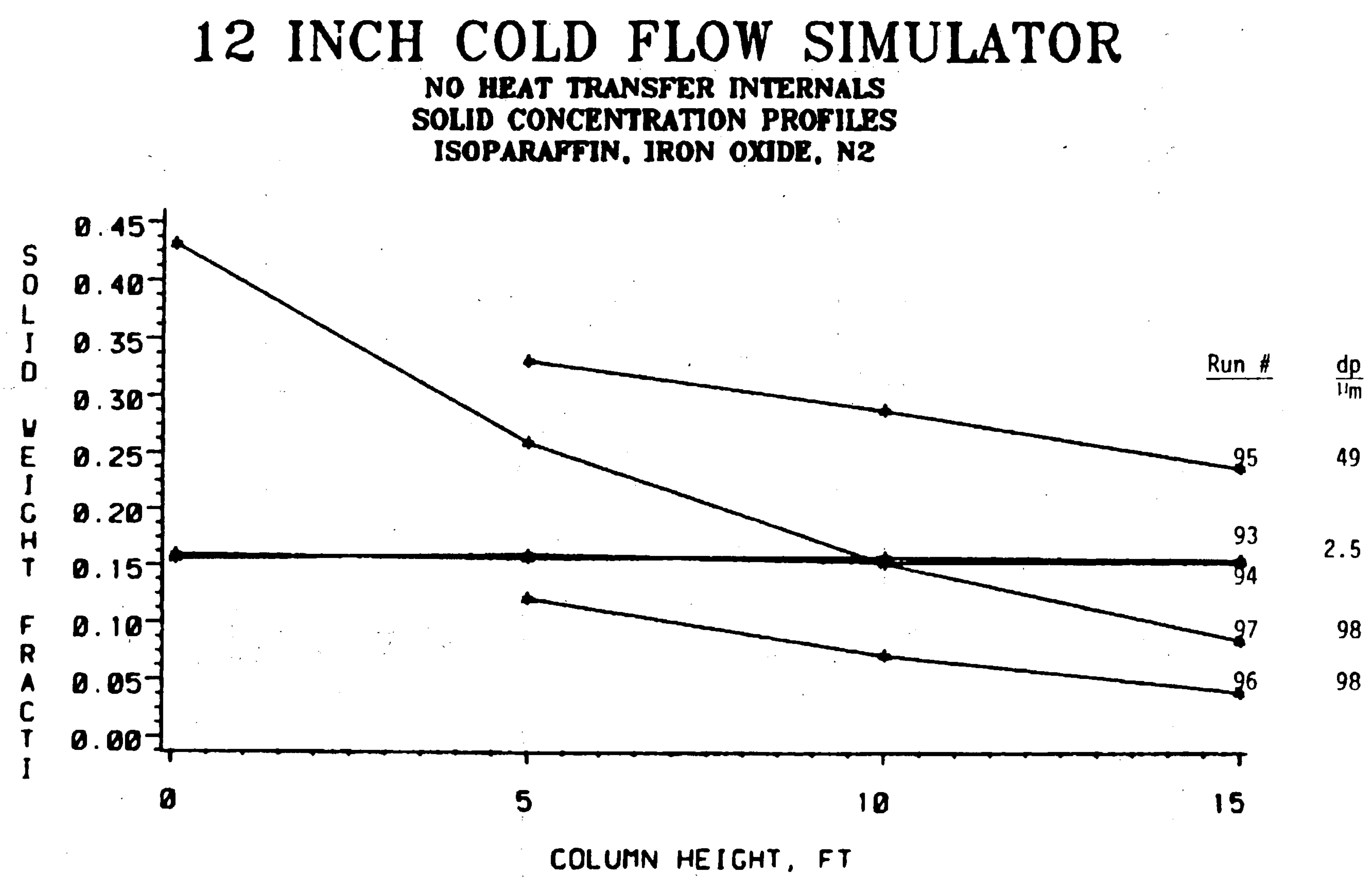

12 INCH COLD FLOW SIMULATOR
NO HEAT TRANSFER INTERNALS
SOLID CONCENTRATION PROFILES
ISOPARAFFIN, IRON OXIDE, N2
SOLID WEIGHT FRACTI
0.45
0.40
0.35
0.30
0.25
0.20
0.15
0.10
0.05
0.00
0
5
10
15
COLUMN HEIGHT, FT
Run #
dp μm
95
49
93
94
2.5
97
98
96
98

Figure 4

Calibration Chamber

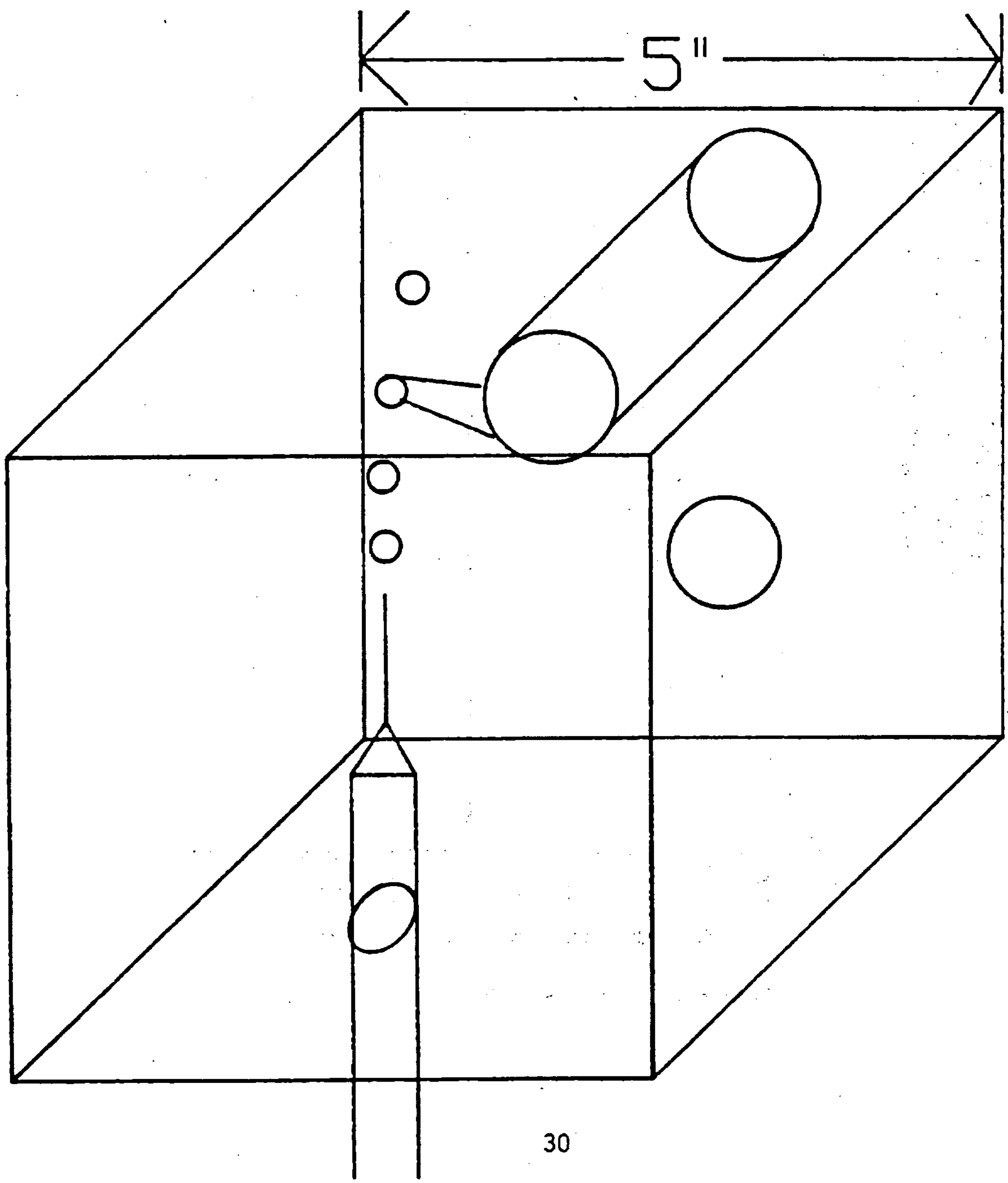

Figure 5

BUBBLE TRACE FROM DOUBLE CONE PROBE

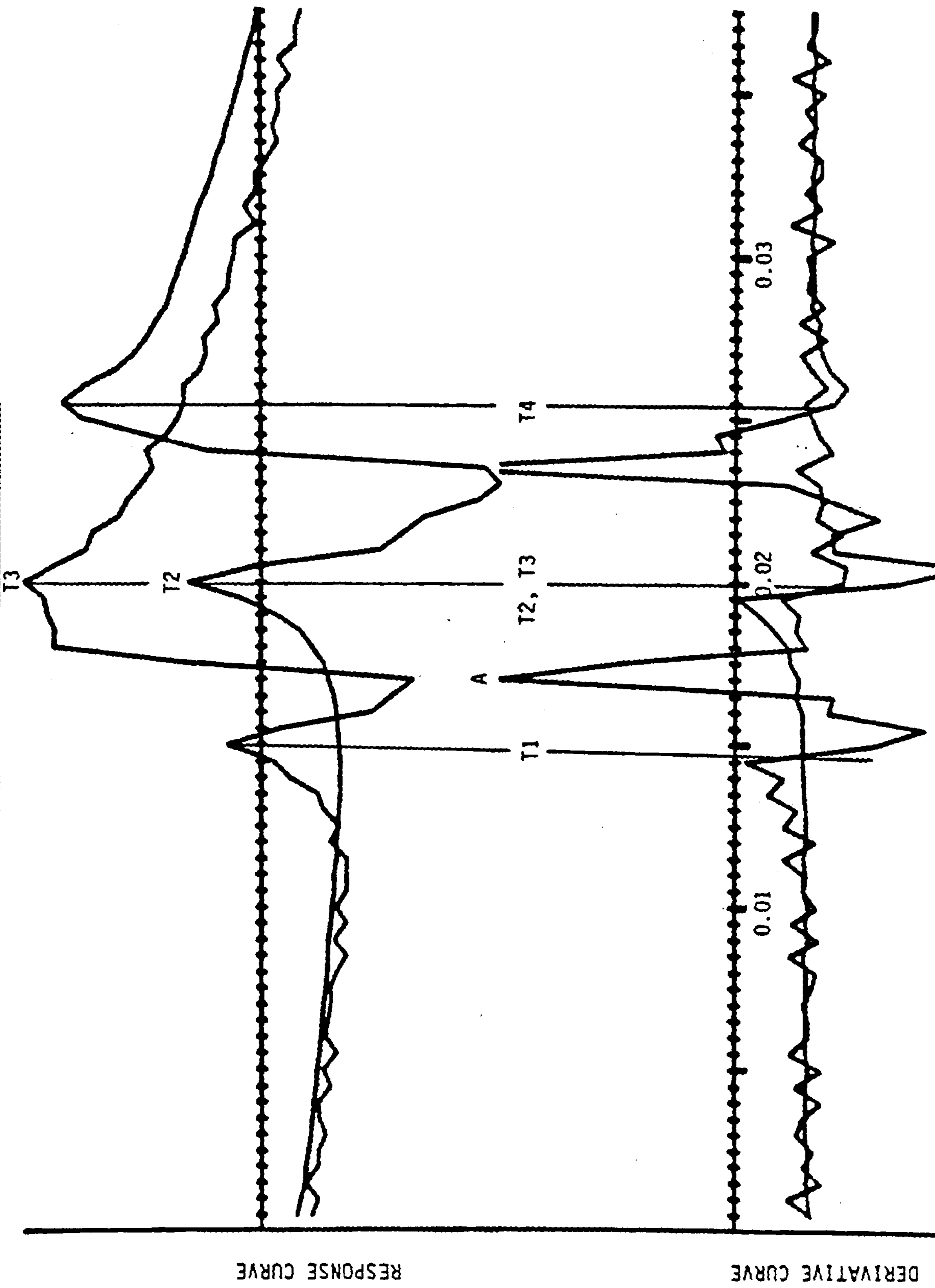

☆U S GOVERNMENT PRINTING OFFICE 1985-544-063/ 107